Applied and Environmental Microbiology, Sept. 2011, p. 6636–6643 Vol. 77, No. 18
0099-2240/11/$12.00 doi:10.1128/AEM.05780-11

New Nystatin-Related Antifungal Polyene Macrolides with Altered Polyol Region Generated via Biosynthetic Engineering of *Streptomyces noursei*▽†

Trygve Brautaset,[1]# Håvard Sletta,[1]# Kristin F. Degnes,[1] Olga N. Sekurova,[2,3] Ingrid Bakke,[2,3] Olga Volokhan,[3] Trygve Andreassen,[2] Trond E. Ellingsen,[1] and Sergey B. Zotchev[2,3]*

Department of Biotechnology, SINTEF Materials and Chemistry, N-7465 Trondheim, Norway[1]; Department of Biotechnology, Norwegian University of Science and Technology, N-7491 Trondheim, Norway[2]; and Biosergen AS, N-7465 Trondheim, Norway[3]

Received 8 June 2011/Accepted 8 July 2011

Polyene macrolide antibiotics, including nystatin and amphotericin B, possess fungicidal activity and are being used as antifungal agents to treat both superficial and invasive fungal infections. Due to their toxicity, however, their clinical applications are relatively limited, and new-generation polyene macrolides with an improved therapeutic index are highly desirable. We subjected the polyol region of the heptaene nystatin analogue S44HP to biosynthetic engineering designed to remove and introduce hydroxyl groups in the C-9–C-10 region. This modification strategy involved inactivation of the P450 monooxygenase NysL and the dehydratase domain in module 15 (DH15) of the nystatin polyketide synthase. Subsequently, these modifications were combined with replacement of the exocyclic C-16 carboxyl with the methyl group through inactivation of the P450 monooxygenase NysN. Four new polyene macrolides with up to three chemical modifications were generated, produced at relatively high yields (up to 0.51 g/liter), purified, structurally characterized, and subjected to *in vitro* assays for antifungal and hemolytic activities. Introduction of a C-9 hydroxyl by DH15 inactivation also blocked NysL-catalyzed C-10 hydroxylation, and these modifications caused a drastic decrease in both antifungal and hemolytic activities of the resulting analogues. In contrast, single removal of the C-10 hydroxyl group by NysL inactivation had only a marginal effect on these activities. Results from the extended antifungal assays strongly suggested that the 9-hydroxy-10-deoxy S44HP analogues became fungistatic rather than fungicidal antibiotics.

Polyene macrolides are important antifungal agents that impose a fast fungicidal effect and have a broad spectrum of activity and a very low tendency of resistance development among fungal pathogens. Their disadvantage, however, is relatively high toxicity, especially toward kidney cells that are especially vulnerable to the hemolytic action of polyene macrolides (2, 24). The latter is related to the mode of action of these antibiotics, which is manifested through the binding of antibiotic molecules to the sterols in eukaryotic membranes (ergosterol in fungal and cholesterol in mammalian). This binding, apparently mediated through conjugated double bonds on the polyene macrolide molecules, eventually leads to the formation of hydrophilic channels (from several antibiotic molecules) lined up on the inside by the hydroxy groups located opposite conjugated double bonds (3, 14, 18). Leakage of ions through these channels is assumed to be responsible for the fungicidal action of polyene macrolides, and some affinity of polyene macrolides to cholesterol is responsible for a similar action on the mammalian cells, manifested by hemolytic activity.

* Corresponding author. Mailing address: Department of Biotechnology, Norwegian University of Science and Technology, N-7491 Trondheim, Norway. Phone: 47 73 59 86 79. Fax: 47 73 59 12 83. E-mail: sergey.zotchev@nt.ntnu.no.

# These authors have contributed equally to this work.

† Supplemental material for this article may be found at http://aem.asm.org/.

▽ Published ahead of print on 15 July 2011.

Nystatin is a polyene macrolide antibiotic produced by *Streptomyces noursei* ATCC 11455 and used in human therapy for treatment of topical fungal infections. Structurally, nystatin is very similar to amphotericin B (AmB), the only polyene macrolide currently approved for treatment of invasive mycoses in humans. AmB has seven conjugated double bonds in its polyene region, while nystatin has four. This difference accounts for the considerably higher antifungal activity of AmB, presumably due to a more efficient hydrophobic interaction with membrane sterols. Numerous attempts to generate less-toxic chemical analogues of AmB have been reported (2). Recently, these have been complemented by a series of genetically engineered amphotericin analogues, some of which showed considerably reduced *in vitro* toxicity (11, 12, 20, 22). We have previously constructed an *S. noursei* mutant, GG5073SP, producing heptaenic nystatin analogue S44HP (4), which displayed considerably improved antifungal activity but also increased hemolytic activity compared to that of nystatin (7). Inactivation of P450 monooxygenase gene *nysN* on the GG5073SP genetic background yielded a mutant strain producing nystatin analogue BSG005 (16-decarboxy-16-methyl-28,29-didehydronystatin). This compound displayed antifungal activity higher than that of S44HP, while its hemolytic activity was somewhat reduced (7).

In this work we report further biosynthetic engineering of nystatin analogues specifically aimed at modification of the polyol region. Theoretically, and according to the current model of the hydrophilic channel created by polyene macrolides in the fungal membrane, the absence or presence of the

TABLE 1. Microbial strains and plasmids used in this study

Strain or plasmid	Relevant genotype[a]	Source or reference
Fungus strain		
Candida albicans ATCC 10231	Indicator fungi, nystatin sensitive	ATCC
Bacterial strains		
E. coli XL1 blue	General cloning host	New England Biolabs
E. coli ET12567 (pUZ8002)	Strain for intergenic conjugation; Km^r, Cm^r	17
S. noursei ATCC 11455	Wild type, nystatin producer	ATCC
S. noursei NG7	Mutant (nitrosoguanidine) of *S. noursei* ATCC 11455, nystatin overproducer	12
S. noursei GG5073SP	ER5 mutant producing nystatin analogue S44HP	4
S. noursei BSM1	ER5 *nysN* double mutant producing nystatin analogue BSG005	7
S. noursei NLD101	NDA59 with in-frame deletion of the *nysL* gene	19
S. noursei BSM11	ER5 *nysL* double mutant producing nystatin derivative BSG022	This work
S. noursei BSM12	ER5 *nysL nysN* triple mutant producing nystatin derivative BSG019	This work
S. noursei BSM13	ER5 DH15 double mutant producing nystatin derivative BSG003	This work
S. noursei BSM14	ER5 DH15 *nysN* triple mutant producing nystatin derivative BSG018	This work
S. noursei BSM14_NG7	Analogous to mutant BSM14 but with ER5, DH15, *nysN* mutations introduced into NG7 genetic background, BSG018 overproducer	This work
Plasmids		
pSOKER5mutGG121SP	Plasmid for introduction of GG5073SP mutation in the ER5 coding region, Am^r	4
pNA0	Plasmid for *nysA* complementation, Am^r	6
pKOnysNCL346ST	Plasmid for *nysN* inactivation, Am^r	7
pSH15-123	Plasmid for DH15 inactivation, Am^r	7
pNLD1	*nysL* replacement vector	19
pNLD2	pNLD1 with CL346AS mutation in *nysN* coding region	This work

[a] Km^r, kanamycin resistance; Cm^r, chloramphenicol resistance; Am^r, apramycin resistance.

hydroxy groups facing the inside of the channel should influence its conductivity for ions and thus antifungal and hemolytic activities. Using genetic engineering, we obtained four new nystatin analogues with added or/and removed hydroxy groups in the polyol region. These modifications were also combined with the replacement of an exocyclic carboxyl with a methyl group. Evaluation of these analogues in terms of antifungal and hemolytic activities provided new insights into the structure-activity relationship of polyene macrolides.

MATERIALS AND METHODS

Microbial strains and plasmids, growth conditions, and DNA manipulations. Microbial strains and plasmids used in this study are listed in Table 1. *Escherichia coli* strains were cultivated in LB medium, supplemented with chloramphenicol (20 μg/ml), apramycin (50 μg/ml), and kanamycin (50 μg/ml) as appropriate. Gene replacements were performed by conjugations to *S. noursei* strains, and selection of double homologous recombination was performed as described previously (21). Standard DNA techniques, including PCR, Southern hybridizations, site-directed mutagenesis, and DNA sequencing were performed essentially as described previously (7).

Construction of *S. noursei* mutant strains. (i) BSM11. Several attempts to introduce the *nysL* mutation, by using the *nysL* deletion plasmid pNLD1, into the *S. noursei* mutant GG5073SP by double homologous recombination failed for unknown reasons. Therefore, we used previously constructed *S. noursei nysL* mutant strain NLD101 (23) as a genetic background for the introduction by double homologous recombination of the enoyl reductase 5 (ER5) mutation by the use of plasmid pSOKER5mutGG121SP (4). The resulting strain, designated BSM11, is an *nysL* ER5 double mutant.

(ii) BSM12. *S. noursei* mutant strain BSM1 (7) was used as the genetic background for the introduction of an *nysL* mutation. Due to the close proximity of the *nysL* and *nysN* genes on the *S. noursei* chromosome (5), a modified version of the *nysL* inactivation plasmid pNLD1 (23) was constructed to avoid reversion of the chromosomal *nysN* mutation in this strain. More specifically, the mutagenic oligonucleotides CL346AS-F and CL346AS-R were used to introduce the CL346AS mutation in the NysN active site coding region of pLND1 by using site-directed mutagenesis as described elsewhere (7). The resulting modified vector pNLD2 was introduced into BSM1 by double homologous recombination, yielding a recombinant strain, BSM12, with the ER5 *nysL nysN* mutations.

(iii) BSM13. ER5 inactivation vector pSOKER5mutGG121SP was introduced to *S. noursei* mutant strain NJDH15 (7) by double homologous recombination. The resulting strain was designated BSM13 and is an ER5 DH15 double mutant.

(iv) BSM14. The previously constructed *nysN* inactivation vector pKOnysN-CL346AS (7) was introduced to *S. noursei* mutant strain BSM13, described above, by double homologous recombination. The resulting strain is an ER5 DH15 *nysN* triple mutant and was designated BSM14.

(v) BSM14_NG7. The nystatin-overproducing classical *S. noursei* mutant NG7 (16) was used here as an alternative host to improve production levels of nystatin analogues generated by genetic engineering. Initially ER5 inactivation plasmid pSOKER5mutGG121SP was introduced to NG7 by double homologous recombination, yielding strain NG7-ER5. Next, NG7-ER5 was used as a host for the introduction of *nysN* inactivation plasmid pKOnysN-CL346AS by double homologous recombination, resulting in strain NG7-ER5-NysN. Finally, strain NG7-ER5-NysN was used as a host for introducing *nysL* deletion plasmid pNLD2 (see above) by double homologous recombination. The resulting ER5 *nysN nysL* triple mutant strain was designated BSM14_NG7.

All the constructed *S. noursei* strains were verified by Southern analysis and PCR-assisted DNA sequencing to confirm the expected chromosomal mutations. Thereafter, the strains were complemented with *nysA* (except for BSM14_NG7) to restore polyene production as described previously (6).

Production, purification, and analysis of polyenes. The production of polyene analogues and analysis of the products were performed essentially as described elsewhere (4, 7). Cultivations of recombinant *S. noursei* strains were performed in fed-batch fermentation with 2× SAO-50 medium. The production yield (average of a minimum of seven independent productions for BSM11, BSM12, BSM13, and BSM14_NG7 and two independent productions for NG7-ER5 and NG7-ER5-NysN) and purity of the engineered polyenes were determined by liquid chromatography-diode array detector-mass spectrometry (LC-DAD-MS) using the AMB standard (USP) as a reference, assuming that molar extinction coefficients in the spectral regions of interest (386 nm) were unaltered. Materials used in the *in vitro* bioassays were purified by organic extraction, fractionated precipitation of the active principle, and repeated extractions of impurities with

nonpolar solvents. Materials used in the nuclear magnetic resonance (NMR) analysis were obtained by LC-MS-guided high-pressure LC (HPLC) purification as described elsewhere (7, 9). Accurate mass determination was performed by LC-DAD-time of flight (TOF) MS as described previously (7, 9).

***In vitro* assays for determination of antifungal and hemolytic activities.** Determination of *in vitro* antifungal activity was performed essentially as described previously (7, 17). Indicator *Candida albicans* cells were grown in 96-well plates, and cell growth was monitored in the presence of 24 different concentrations of antibiotics. Purity of the active principle of interest was determined using LC-DAD-MS, and the concentration was adjusted according to the purity. MIC values after 22-h incubation of *Candida albicans* were determined from at least 3 parallel experiments.

In order to obtain a better understanding of the antifungal properties of the molecules, we also performed extended antifungal assays determining MIC values for a number of different incubation times of *C. albicans*, ranging from 9 to 22 h. These assays also included tests for discriminating between fungistatic and fungicidal properties. The latter was done by testing for the viability of *C. albicans* cells by plating on agar medium after 20-h incubation with antibiotic concentrations ranging from zero to up to 13× MIC (19).

For the determination of hemolytic activities, the purified antibiotics were subjected to *in vitro* assays monitoring their abilities to cause lysis of defibrinated horse blood erythrocytes, as described previously (7). Based on the obtained data, hemolytic concentrations causing 50% hemolysis (HC_{50} values) were determined, and the results presented are mean values from 3 independent experiments.

Structure determination by NMR. NMR spectra were recorded on a Bruker Avance 600-MHz spectrometer fitted with a TCI cryoprobe. The solvent used was dimethyl sulfoxide (DMSO)-d_6, and chemical shifts are calibrated relative to the residual DMSO signals at 2.50 ppm for ^{1}H and 39.51 ppm for ^{13}C. Peak assignments were performed with the aid of the in-phase correlation spectroscopy (IP-COSY), rotating-frame Overhauser enhancement spectroscopy (ROESY), heteronuclear single-quantum coherence (HSQC), heteronuclear multiple-bond correlation (HMBC), and HSQC-total correlation spectroscopy (TOCSY) experiments.

RESULTS AND DISCUSSION

Rearrangement of the hydroxyl groups at the C-9–C-10 region of S44HP leads to dramatic changes in antifungal and hemolytic activities. We have previously constructed DH15 mutant strain NJDH15, producing nystatin analogue BSG002 (9-hydroxy-10-deoxynystatin), displaying a 2-fold-lower hemolytic activity and a 4-fold-lower antifungal activity than nystatin (7). It was of interest to investigate if the combination of DH15 and ER5 inactivation (the latter yielding a heptaene analogue with significantly increased activity [4]) could generate an antibiotic with overall improved MIC-versus-HC_{50} properties. We have previously reported that NysL is unable to perform the C-10 hydroxylation of BSG002, presumably due to the high substrate specificity for the nystatin C-9-to-C-11 region (7). We here introduced the ER5 mutation GG5073SP into the NJDH15 mutant, and the resulting recombinant strain BSM13 was cultivated in the fed-batch fermentation. The accurate mass of the main polyene compound in the DMSO extract of the fermentation broth was determined by LC-DAD-TOF. As expected, the analysis revealed the production of an analog with a mass (*m*/*z*) corresponding to the stoichiometric formula $C_{47}H_{73}N_1O_{17}$ in negative-mode electrospray ionization (ESI^-) (0.3-ppm difference from the theoretical mass) (see Fig. S1S in the supplemental material). The measured accurate mass is the same as that for S44HP, but the altered retention time during chromatography suggested that a different compound was produced. The new molecule, designated BSG003, was suggested to be 9-hydroxy-10-deoxy-S44HP, as shown in Fig. 1, and its molecular structure was confirmed by NMR (see below). The volumetric production yield of BSG003 and the purity of the sample used in the bioassays are given in Table 2.

In vitro analyses of BSG003 (concentration of active principle adjusted according to the purity) revealed that this compound displayed an about-60-fold-increased MIC value compared to that of the parental molecule S44HP (Table 3). Interestingly, very low hemolytic activity was measured for all BSG003 concentrations tested, and the HC_{50} value of BSG003 was determined to be >200-fold increased compared to that of S44HP (Table 3). These data suggested that the introduction of a C-9 hydroxyl and the concomitant removal of the C-10 hydroxyl have a pronounced negative effect on the antifungal activity, while reducing the hemolytic properties of S44HP even more strongly. These results suggested that C-9 methylene, C-10 hydroxyl, or both moieties in the polyol region strongly affect the biological properties of nystatin and its derivatives.

Based on the dramatically increased HC_{50} value of BSG003 compared to that of S44HP, it was of interest to introduce the analogous polyol modification into BSG005 in an attempt to improve the already favorable MIC-versus-HC_{50} properties of this nystatin analogue (7). Accordingly, the *nysN* inactivation plasmid pKOnysN-CL346AS was introduced into the BSM13 mutant, and the resulting recombinant strain BSM14 was cultivated in the fed-batch fermentor for polyene production. However, due to the very poor polyene production yields in BSM14 (data not shown), the purification and concomitant polyene characterizations were not possible.

Therefore, we constructed an analogous ER5 DH15 NysN mutant strain by using the nystatin-overproducing strain *S. noursei* NG7 as a genetic background (12). This strategy involved the successive introduction of three individual chromosomal mutations in the ER5, NysN, and DH15 coding regions (see Materials and Methods), and the respective polyene production levels were verified for each introduced mutation. Strain NG7-ER5 produced S44HP at a substantially higher level (ca. 7-fold) than that of the wild type-based *S. noursei* GG5073SP strain (Table 2). Next, NG7-ER5 was used as a host for the introduction of the *nysN* mutation. The resulting NG7-ER-NysN mutant produced nystatin analogue BSG005 at an about-8-times-higher volumetric yield than the BSG005 production level for the previously constructed wild-type-based mutant BSM1 (Table 2). Finally, the NG7-ER5-NysN mutant was used as a host for the introduction of the DH15 mutation. The resulting triple mutant strain, designated BSM14_NG7, was then cultivated in a fed-batch fermentor, and produced polyene macrolides were analyzed in the DMSO extract of the fermentation broth. The accurate mass of the main polyene macrolide determined by LC-DAD-TOF analysis corresponding to the stoichiometric formula expected for a 9-hydroxy-10-deoxy BSG005 analogue ($C_{47}H_{75}N_1O_{15}$) was detected in the ESI^- (negative-ionization) mode (less than 0.3-ppm difference from the theoretical mass). The presence of chlorine adducts gave additional support to the determination of the correct molecular weight of this heptaene compound, which was partly fragmented during ionization, yielding fragment ions with *m*/*z* values 18 and 36 lower than that of the parent ion. This represents losses of one and two H_2O, respectively, which are common neutral losses in the MS-ESI analyses (see Fig. S1S in the supplemental material). The new molecule was designated

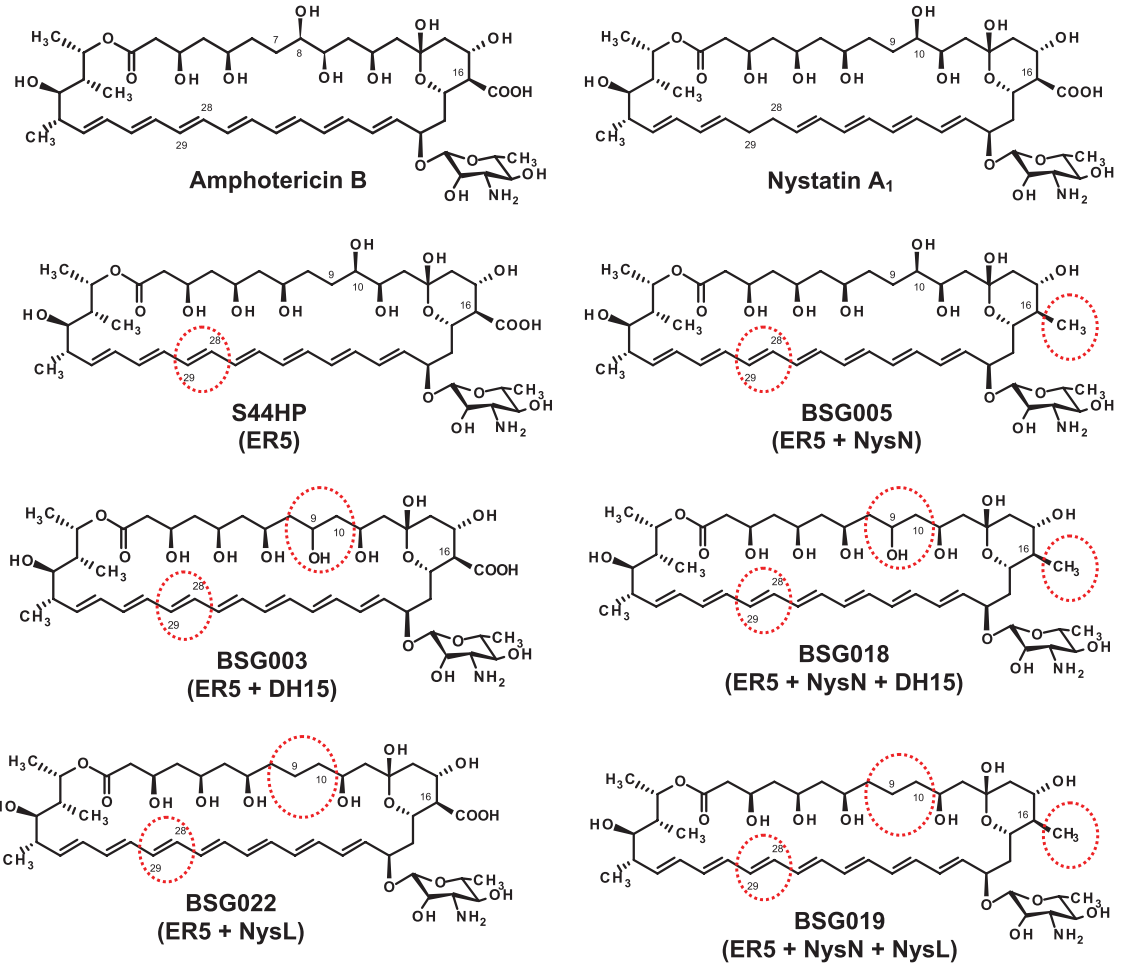

FIG. 1. Molecular structures of amphotericin B, nystatin A_1, heptaene nystatin derivatives S44HP and BSG005, and their analogues generated by genetic engineering. Red circles indicate chemical modifications relative to nystatin A_1, and the corresponding mutations are given under the respective molecule names.

BSG018, and its structure is shown in Fig. 1. The volumetric production yield of BSG018 and purity of the sample used in the bioassays are given in Table 2.

In vitro analyses of BSG018 (concentration of active principle adjusted according to the purity) demonstrated that the MIC value for this compound was increased over 80-fold compared to that of BSG005 (Table 3). Moreover, no significant hemolytic activity could be detected with BSG018 under the conditions tested (Table 3), indicating that the HC_{50} value for this compound is dramatically increased (over 50-fold) compared to that for BSG005. Together, these results were in agreement with the data obtained for BSG003 and confirmed that oxidation of the C-9 methylene and removal of the C-10 hydroxyl dramatically reduced both the antifungal and hemolytic activities of nystatin analogues under the conditions tested.

TABLE 2. Identity, yield, and purity of the newly generated nystatin analogues

Molecule	Mutant (mutation)	Yield (g/liter)	Purity (%)[a]	Reference or source
S44HP	GG5073SP (ER5)	1.28 ± 0.07	95	7
S44HP	NG7-ER5 (ER5)	9.1 ± 0.4	ND	This work
BSG005	BSM1 (ER5 *nysN*)	0.53 ± 0.01	95	7
BSG005	NG7-ER5-NysN (ER5 *nysN*)	3.9 ± 0.1	ND	This work
10-Deoxynystatin	NLD101 (*nysL*)	1.06 ± 0.04	95	19
BSG003	BSM13 (ER5 DH15)	0.51 ± 0.02	80	This work
BSG018	BSM14_NG7 (ER5 DH15 *nysN*)	0.24 ± 0.02	74	This work
BSG019	BSM12 (ER5 *nysN nysL*)	0.47 ± 0.03	90	This work
BSG022	BSM11 (ER5 *nysL*)	0.29 ± 0.02	87	This work

[a] ND, not determined during this study.

TABLE 3. *In vitro*-determined antifungal and hemolytic activities of the genetically engineered S44HP analogues[d]

Compound	Mutation(s)	MIC (μg/ml)[a]	HC_{50} (μg/ml)[b]
AmB	None	0.18 ± 0.03	3.0 ± 0.25
S44HP	ER5	0.19 ± 0.03	3.0 ± 0.25
BSG005	ER5 NysN	0.11 ± 0.03	4.0 ± 0.3
BSG003	ER5 DH15	12.0 ± 0.60	>600[c]
BSG018	ER5 NysN DH15	9.0 ± 0.45	>200[c]
BSG022	ER5 NysL	0.20 ± 0.02	1.4 ± 0.15
BSG019	ER5 NysN NysL	0.12 ± 0.03	4.5 ± 0.3

[a] Tested as described in reference 7, using *C. albicans* as test organism and with 22-h exposure time.

[b] Tested as described in reference 7, using defibrinated horse blood cells and antibiotic concentrations ranging between 0 and 600 μg/ml.

[c] For BSG003, 13% hemolysis was observed at the highest concentration tested (600 μg/ml); for BSG018, 3% hemolysis was observed at the highest concentration tested (200 μg/ml).

[d] The ± values represent maximum deviation from the mean.

Removal of the C-10 hydroxyl from S44HP analogues has marginal effects on antifungal and hemolytic activities. In order to determine whether the effect on biological activity observed for the BSG003 and BSG018 molecules was due to the changes at C-9 or C-10, we decided to remove a single C-10 hydroxyl from the S44HP and BSG005 analogues. In a previous report we demonstrated that inactivation of the P450 mono-oxygenase gene *nysL* in *S. noursei* resulted in a mutant strain, designated NLD101, which produced 10-deoxynystatin with antifungal activity similar to that of the parental antibiotic nystatin (23). However, the hemolytic activity of 10-deoxynystatin has not been tested. To explore the effect of the C-10 hydroxyl removal further, we used mutant strain NLD101 as a genetic background for inactivation of the NysC enoyl reductase domain ER5 responsible for the appearance of the C-28–C-29 saturated bond on the nystatin molecule (5). The resulting mutant strain BSM11 was cultivated in fed-batch fermentors, and DMSO extracts of fermented broth were analyzed for production of polyene macrolides. The accurate mass of the main polyene macrolide was determined by LC-DAD-TOF, and the measured mass (*m/z*) in ESI^- (negative-ionization) mode corresponded well with the expected stoichiometric formula $C_{47}H_{73}N_1O_{16}$ of 10-deoxy-S44HP (1.5-ppm difference from the theoretical mass) (see Fig. S1S in the supplemental material). The new molecule was designated BSG022, and its chemical structure is shown on Fig. 1. The volumetric production yield of BSG022 and purity of the sample used in the bioassays are given in Table 2.

Next, BSG022 (concentration of active principle adjusted according to the purity) was assayed for antifungal and hemolytic activities, and the results are presented in Table 3. The MIC value of BSG022 was similar to that of S44HP (Table 3), indicating that the C-10 hydroxyl removal had no significant effect on the antifungal activity, which was in agreement with the previous report on 10-deoxynystatin (23). The HC_{50} value of BSG022 was more than 2-fold reduced compared to that of S44HP, suggesting increased toxicity to erythrocytes. Summarized, these data implied that the C-10 hydroxyl group is not critical for the antifungal activity, while removal of this group causes a moderate increase in the hemolytic activity of S44HP under the conditions tested.

We previously inactivated the P450 monooxygenase gene *nysN* in *S. noursei*, leading to the production of 16-decarboxy-16-methyl nystatin (16-DecNys) with 2-fold reduced hemolytic activity and retained antifungal activity compared to nystatin (7). Analogous inactivation of *nysN* in the GG5073SP genetic background gave mutant strain BSM1, producing the nystatin analogue BSG005, which, in contrast to 16-DecNys, displayed improved antifungal and hemolytic activity compared to that of the parental molecule S44HP (7). These data demonstrated that the effect of single modifications may depend on the type of polyene molecule, and we therefore proceeded to inactivate *nysL* in the BSM1 mutant in order to remove the C-10 hydroxyl from the BSG005 polyol region. The *nysL* and *nysN* genes are clustered on the *S. noursei* chromosome (5). Therefore, alternative *nysL* inactivation vector pNLD2 carrying the *nysN* CL346AS mutation was constructed and used to inactivate the *nysL* coding region in BSM1 without reversing the chromosomal *nysN* CL346AS mutation already present in this host. The resulting recombinant *S. noursei* strain, designated BSM12, was cultivated in fed-batch fermentation as described above, and the DMSO extract of the broth was subjected to analysis. The accurate mass of the main polyene macrolide in the extract was determined by LC-DAD-TOF, and the measured mass (*m/z*) in ESI^- corresponded well with the expected stoichiometric formula $C_{47}H_{75}N_1O_{14}$ (0.1-ppm difference from the theoretical mass) of 10-deoxy-BSG005. The presence of acetate adducts gave additional support to the determination of the correct molecular weight of this heptaene compound. The compound is partly fragmented during ionization, yielding fragment ions with *m/z* values 18 lower than the parent ion. This represents losses of one H_2O, which are common neutral losses in MS-ESI analyses (see Fig. S1S in the supplemental material). The new molecule designated BSG019 was concluded to be the expected 10-deoxy-16-decarboxy-16-methyl-28,29-didehydronystatin (10-deoxy-BSG005 in Fig. 1). The volumetric production yield of BSG019 and the purity of the sample used in the bioassays are given in Table 2. The molecular structure of BSG019 was also confirmed by NMR (see below).

Purified BSG019 (purity above 90% of the total polyenes) was assayed for *in vitro* antifungal and hemolytic activities, and MIC and HC_{50} values of BSG019 were found to be similar to those of BSG005 (Table 3).

Taken together, the *in vitro* data for BSG022 and BSG019 demonstrated that removal of the C-10 hydroxyl group has marginal effects on MIC and hemolytic properties. Considering the data obtained for BSG003 and BSG018, the C-9 methylene in the polyol region of S44HP and BSG005 seems to be important for the biological activity of these molecules either on its own or in combination with C-10 hydroxyl.

Structure elucidation of BSG003 and BSG019 by NMR. The molecular structures of nystatin analogues S44HP, BSG002, and BSG005 have been determined previously by NMR (7, 9), and in the present study analogues BSG003 and BSG019 were chosen as representative candidates for NMR analysis. In general, the ^1H and ^{13}C chemical shifts of both BSG003 and BSG019 (data not shown) had a strong resemblance to those of related polyene macrolides recorded for DMSO-d_6, like AmB (1, 8). Assignments of chemical shifts for both structures could be established by tracking ^1H-^1H correlations along the macrocycle interrupted only by the quaternary positions C-1 and

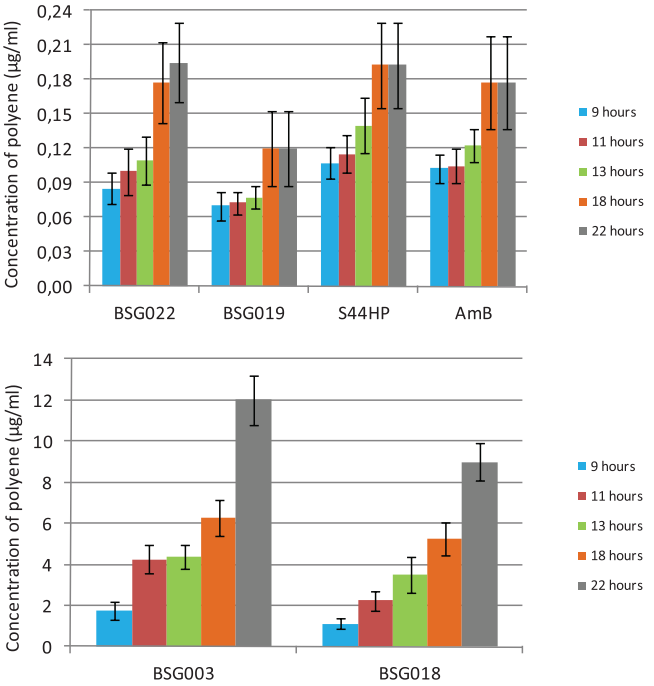

FIG. 2. Schematic representation of MIC values of nystatin analogues obtained after different time periods of *C. albicans* exposure to the antibiotics. *C. albicans* cells were incubated in the presence of different antibiotic concentrations, and cell growth was monitored after 9 h and until 22 h, and the respective MIC values are given. The data for the NysL mutant analogues (BSG022 and BSG019) and AmB and S44HP (top) and the DH15 mutant analogues (BSG003 and BSG018) (bottom) are presented. Different scales on the *y* axes are due to considerable differences in the MIC values between these two classes of molecules at all time points.

C-13. This was aided by HSQC and HSQC-TOCSY experiments which also allowed the assignment of ^{13}C shifts (see Table S1S in the supplemental material). Signals in the central polyene region could not be assigned due to severe overlap. For BSG019, the remaining quaternary ^{13}C signals could be determined from an HMBC experiment. Due to the lower concentration of BSG003 in the NMR sample, HMBC could show couplings only to hydrogen nuclei on methyl groups. Additionally for BSG003, direct ^{13}C observation proved difficult, compelling the use of HSQC for determining the ^{13}C shifts. As a consequence, quaternary signals were not detected for this compound. The recorded shifts are compatible with the suggested structures.

The large coupling constants found for protons 15 and 17 are indicative of axial orientations. This was further supported by a strong nuclear Overhauser effect (NOE) transfer between these nuclei, confirming the relative configuration of C-15–C-17. The relative configuration of the mycosamine group could be confirmed from the large couplings to proton 4′, placing protons 3′, 4′, and 5′ in axial orientations, while small coupling between protons 2′ and 3′ and strong NOE transfer between protons 1′, 3′, and 5′ put protons 1′ and 2′ in axial and equatorial orientations, respectively. In conclusion, the results of these NMR analyses were in agreement with the corresponding LC-DAD isoplot and MS-TOF spectra of these compounds (see Fig. S1S in the supplemental material) and confirmed the chemical structures of BSG003 and BSG019 as presented in Fig. 1.

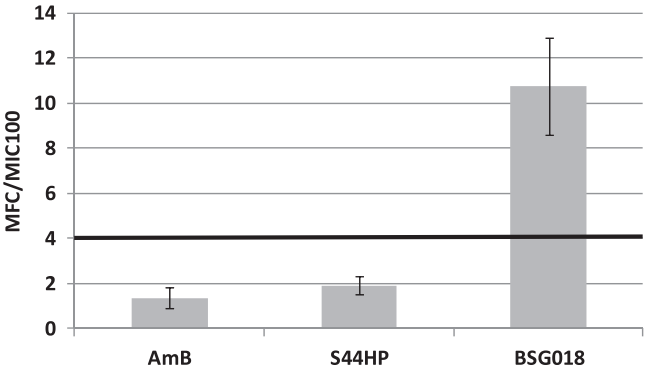

FIG. 3. Ratio of the minimum fungicidal concentration (MFC) to the MICs of the polyene macrolides tested on *C. albicans* (MFC/MIC) (see Materials and Methods). The MFC of each polyene macrolide was determined from the average of the highest polyene concentration for which colonies appeared on the agar plates and the lowest concentration for which no colonies appeared. The area below the bold line represents an MFC/MIC ratio of <4, typical for fungicidal antibiotics (15).

9-Hydroxy-10-deoxy S44HP analogues display fungistatic properties. To distinguish between the fungicidal (cell killing) and fungistatic (growth inhibition) activities among different analogues, the *in vitro* antifungal assays were extended to also include growth measurements at several additional incubation times (9, 11, 13, 18, and 22 h). The results obtained are summarized in Fig. 2. The two analogues lacking, compared to S44HP, the C-10 hydroxyl group (BSG022 and BSG019) displayed inhibition patterns similar to those of the control antibiotics S44HP and AmB, for which calculated MIC values did not increase much (ca. 2-fold) with prolonged incubation. These data indicate efficient killing of the yeast cells at all incubation times tested. In contrast, the two analogues BSG003 and BSG018, carrying C-9 hydroxyl and lacking C-10 hydroxyl, displayed significantly different inhibition patterns. For these two molecules, the MIC values increased 7-fold and 12-fold, respectively, when incubation time was increased from 9 h to 22 h. These data suggested that BSG003 and BSG018 either exhibited fungistatic rather than fungicidal properties or were highly unstable.

To investigate this further, we tested *C. albicans* cells for survival after 20-h incubation, with antibiotic concentrations ranging from zero to up to 13-fold the respective MICs as described by Pannu et al. (19). Cultures were thereafter directly plated on solid agar medium, and viable cells were scored for the appearance of colonies within 24 h of incubation. The results demonstrated that both AmB and S44HP were clearly fungicidal, as no colonies were obtained with antibiotic concentrations of 1 to 1.5× MIC or higher. In contrast, in the case of BSG018, colonies appeared for all the tested concentrations up to 8.6× MIC (Fig. 3). These data strongly supported the assumption that the 9-hydroxy-10-deoxy analogues of S44HP became fungistatic antibiotics. We could, however, not rule out the possibility that some of the data obtained in these experiments may be due to the low chemical stability of BSG018 under the conditions tested. Therefore, both the whole cultures and the supernatants from the BSG018-exposed cultures were analyzed by LC-DAD-MS to

quantify the amount of BSG018 remaining after 20-h incubation. The results obtained (see Fig. S2S in the supplemental material) clearly demonstrated that BSG018 was present in the cultures at concentrations significantly exceeding the MIC for initial exposure concentrations >4× MIC. The analyses also showed that BSG018 was present in soluble form in cell-free supernatants of the exposed cultures for all concentrations tested. Thus, the observed fungistatic properties of BSG018 were most likely due to the introduced C-9 and C-10 modifications and not because of the molecule's chemical instability in the cultures.

Structurally similar polyene macrolide amphotericin B is known to form two types of channels in the biological membranes (14). The first type, called nonaqueous channels, is formed at low AmB concentrations, and these channels are permeable to small nonelectrolytes and hydrated monovalent ions (13, 15). Since these channels do not pierce the membrane and do not allow leakage of electrolytes, their formation is likely to be nonlethal for the fungal cell. The second type, called aqueous pores, are formed at an increased antibiotic concentration and span the membrane layer completely, allowing leakage of electrolytes and big molecules, such as glucose (14). Formation of the latter channels would definitely have a very significant effect on fungal cell viability, hence making AmB fungicidal. The structure of the polyene macrolide molecule might have a drastic effect on the mechanism of channel formation, which is currently envisaged as horizontal positioning of antibiotic monomers at the membrane-water interface followed by membrane penetration (14). The latter step, however, is difficult to imagine without a conformational change in the polyene macrolide molecule allowing a temporary kink in the ring structure, facilitating membrane penetration. Such a kink is possible for the polyene macrolides with at least one CH_2-CH_2 moiety, allowing some degree or rotation around this bond in the polyol region. Such moieties are indeed present in the polyol regions of AmB (C-6 and C-7) and some nystatin analogues, including S44HP and BSG005 (C-8 and C-9). However, replacement of one of the hydrogens in C-9 methylene with a hydroxyl group, such as in BSG003 and BSG018, significantly changes the polyol environment. The KR15 domain in NysJ is of the B type, and according to Caffrey (10), inactivation of DH15 shall lead to the appearance of a C-9 alcohol in a configuration identical to those of other hydroxyl groups in the polyol region, i.e., above the ring plane. From this point of view, the repositioning of a hydroxyl group from C-10 to C-9, as it happens in BSG003 and BSG018, brings it into the proximity of the neighboring hydroxyls at C-7 and C-11. Such a repositioning creates a perfect lineup of the hydroxyl groups in the polyol region, which is favorable for hydrogen bond formation and, consequently, an increase in the rigidity of the macrolactone ring. Since the rotation around the C-8–C-9 bond becomes more restricted, the kinking of the BSG003 and BSG018 molecules necessary for the membrane penetration becomes problematic. Possibly, due to such a conformational constraint, these antibiotics can form only nonaqueous channels, which would have a fungistatic, but not a fungicidal, effect on fungal cells.

Conclusions. Four new heptaene nystatin analogues with alterations in the C-9–C-10 portion of the polyol region and C-16 exocyclic carboxyl group were generated via biosynthetic engineering of *S. noursei*. Biological testing of the new analogues revealed the significant negative effect of the repositioning of the C-10 hydroxyl to the C-9 position on both antifungal and hemolytic activities. At the same time, the removal of C-10 hydroxyl alone did not seem to have any effect on the antifungal activity but increased the hemolytic activity. Interestingly, replacement of the C-16 carboxyl with a methyl group on the molecules with a modified C-9–C-10 region appears to increase the antifungal activity while reducing the hemolytic activity. Molecules with a C-10-to-C-9-repositioned hydroxyl group were found to have strongly reduced fungicidal activity and became fungistatic antibiotics, and a plausible explanation of this phenomenon was proposed. Taken together, these data shed new light onto the structure-activity relationship of polyene macrolides and might assist in molecular design aimed at the generation of more effective and safe antifungal drugs for human therapy.

ACKNOWLEDGMENTS

This work was financed by Biosergen AS and by a grant from the Research Council of Norway.

REFERENCES

1. **Aszalos, A., A. Bax, N. Burlinson, P. Roller, and C. McNeal.** 1985. Physicochemical and microbiological comparison of nystatin, amphotericin A, and amphotericin B, and structure of amphotericin A. J. Antibiot. **38:**1699–1713.
2. **Baginski, M., and J. Czub.** 2009. Amphotericin B and its new derivatives—mode of action. Curr. Drug Metab. **10:**459–469.
3. **Baginski, M., J. Czub, and K. Sternal.** 2006. Interaction of amphotericin B and its selected derivatives with membranes: molecular modeling studies. Chem. Rec. **6:**320–332.
4. **Borgos, S. E. F., et al.** 2006. Effect of glucose limitation and specific mutations in the module 5 enoyl reductase domains in the nystatin and amphotericin polyketide synthases on polyene macrolide biosynthesis. Arch. Microbiol. **185:**165–171.
5. **Brautaset, T., et al.** 2000. Biosynthesis of the polyene antifungal antibiotic nystatin in *Streptomyces noursei* ATCC 11455: analysis of the gene cluster and deduction of the biosynthetic pathway. Chem. Biol. **7:**395–403.
6. **Brautaset, T., S. E. Borgos, H. Sletta, T. E. Ellingsen, and S. B. Zotchev.** 2003. Site-specific mutagenesis and domain substitutions in the loading module of the nystatin polyketide synthase, and their effects on nystatin biosynthesis in *Streptomyces noursei*. J. Biol. Chem. **278:**14913–14919.
7. **Brautaset, T., et al.** 2008. Improved antifungal polyene macrolides via engineering of the nystatin biosynthetic genes in *Streptomyces noursei*. Chem. Biol. **15:**1198–1206.
8. **Brown, J. M., and P. J. Sidebottom.** 1981. The proton magnetic resonance spectrum of amphotericin B. Tetrahedron **37:**1421–1428.
9. **Bruheim, P., et al.** 2004. Chemical diversity of polyene macrolides produced by *Streptomyces noursei* ATCC 11455 and recombinant strain ERD44 with genetically altered polyketide synthase NysC. Antimicrob. Agents Chemother. **48:**4120–4129.
10. **Caffrey, P.** 2003. Conserved amino acid residues correlating with ketoreductase stereospecificity in modular polyketide synthases. Chembiochem **4:**654–657.
11. **Caffrey, P., J. F. Aparicio, F. Malpartida, and S. B. Zotchev.** 2008. Biosynthetic engineering of polyene macrolides towards generation of improved antifungal and antiparasitic agents. Curr. Top. Med. Chem. **8:**639–653.
12. **Carmody, M., et al.** 2005. Biosynthesis of amphotericin derivatives lacking exocyclic carboxyl groups. J. Biol. Chem. **280:**34420–34426.
13. **Cohen, B. E.** 1992. A sequential mechanism for the formation of aqueous channels by amphotericin B in liposomes. The effect of sterols and phospholipid composition. Biochim. Biophys. Acta **1108:**49–58.
14. **Cohen, B. E.** 2010. Amphotericin B membrane action: role for two types of ion channels in eliciting cell survival and lethal effects. J. Membr. Biol. **238:**1–20.
15. **Cohen, B. E., and M. Gamargo.** 1987. Concentration and time dependence of amphotericin B-induced permeability changes across plasma membrane vesicles from *Leishmania* sp. Drugs Exp. Clin. Res. **13:**539–546.
16. **Jonsbu, E., M. McIntyre, and J. Nielsen.** 2002. The influence of carbon sources and morphology on nystatin production by *Streptomyces noursei*. J. Biotechnol. **95:**133–144.
17. **Nedal, A., et al.** 2007. Analysis of the mycosamine biosynthesis and attachment genes in the nystatin biosynthetic gene cluster of *Streptomyces noursei* ATCC 11455. Appl. Environ. Microbiol. **73:**7400–7407.

18. **Omura, S., and H. Tanaka.** 1984. Production, structure and antifungal activity of polyene macrolides, p. 351–404. *In* S. Omura (ed.), Macrolide antibiotics: chemistry, biology, and practice. Academic Press, New York, NY.
19. **Pannu, J., et al.** 2009. NB-002, a novel nanoemulsion with broad antifungal activity against dermatophytes, other filamentous fungi, and *Candida albicans*. Antimicrob. Agents Chemother. **53:**3273–3279.
20. **Power, P., et al.** 2008. Engineered synthesis of 7-oxo-and 15-deoxy-15-oxo-amphotericins: insights into structure-activity relationships in polyene antibiotics. Chem. Biol. **15:**78–86.
21. **Sekurova, O., H. Sletta, T. E. Ellingsen, S. Valla, and S. Zotchev.** 1999. Molecular cloning and analysis of a pleiotropic regulatory gene locus from the nystatin producer *Streptomyces noursei* ATCC11455. FEMS Microbiol. Lett. **177:**297–304.
22. **Soler, L., P. Caffrey, and H. E. M. McMahon.** 2008. Effects of amphotericin analogues on the scrapie isoform of the prion protein. Biochim. Biophys. Acta **1780:**1162–1167.
23. **Volokhan, O., H. Sletta, T. E. Ellingsen, and S. B. Zotchev.** 2006. Characterization of the P450 monooxygenase NysL, responsible for C-10 hydroxylation during biosynthesis of the polyene macrolide nystatin in *Streptomyces noursei*. Appl. Environ. Microbiol. **72:**2514–2519.
24. **Zotchev, S. B.** 2003. Polyene macrolide antibiotics and their applications in human therapy. Curr. Med. Chem. **10:**211–223.